Effect of microstructural changes associated with hydrogen damage in API 5L X60 steels

Efecto de los cambios microestructurales asociados al daño por hidrógeno en aceros API 5L X60

Calan-Canche, Damián*[a], Reda-Cruz, Alfredo[b], González-Sánchez, Jorge[c] and Flores-Chan, J.E.[d]

[a] Universidad Autónoma del Carmen • U-3760-2018 • 0000-0001-6688-4468 • 415663
[b] Universidad Autónoma del Carmen • LXW-3806-2024 • 0000-0002-8767-3616 • 952544
[c] Universidad Autónoma del Carmen • LYO-8207-2024 • 0000-0001-5327-5137 • 31164
[d] Universidad Autónoma del Carmen • LXW-4586-2024 • 0000-0003-4714-686X• 175430

CONAHCYT classification: **DOI:** https://doi.org/10.35429/H.2024.14.78.88

Area: Engineering
Field: Engineering
Discipline: Electronic Engineering
Subdiscipline: Electrochemistry

Key Handbooks

Cathodic protection systems are complementary methods used to counteract the corrosion of carbon steel pipeline systems. During the cathodic polarization of the steel in this type of protection methods, hydrogen is generated on the steel surface, which in the best case evolves to molecular hydrogen and is released into the environment. However, part of this generated hydrogen is absorbed in the volume of the steel, causing loss of mechanical properties. In this research work, the microstructure of the steel is modified and the effects on the mechanisms of hydrogen absorption are analyzed. The mechanisms by which hydrogen damage occurs are due to the different environments to which the steel is subjected. Pipelines buried in the ground are mainly in contact with acidic and alkaline media. In acidic environments hydrogen release occurs naturally and in alkaline environments hydrogen release occurs as a consequence of water reduction, this in environments with absence of oxygen. To understand this process, it is essential to relate it to the microstructure present in the steel, which normally has characteristic phases that promote mechanical properties. Very important is the resistance to corrosion in the different media to which the steels are subjected. Modification of the microstructure by quenching heat treatment can be used on an industrial scale because of the associated costs. The quenching heat treatment modifies the mechanisms associated with hydrogen absorption. The microstructure formed consists of different phases of ferrite, bainite and martensite that provide the steel with superior mechanical properties. The heat treatment modifies the corrosion rate with respect to the base material.

Citation: Calan-Canche, Damián, Reda-Cruz, Alfredo, González-Sánchez, Jorge and Flores-Chan, J.E. 2024. Effect of microstructural changes associated with hydrogen damage in API 5L X60 steels. 78-88. ECORFAN.

* ✉ [jodcalan@gmail.com]

Handbook shelf URL: https://www.ecorfan.org/handbooks.php

Abstract

The effect of unconventional heat treatment and electrochemical behavior on API 5L X60 steel is evaluated by electrochemical processes/mechanisms associated with corrosion. The susceptibility to hydrogen absorption in soil solutions representative of the State of Campeche, Mexico, was evaluated. In the energy, chemical, metallurgical/mechanical, and petrochemical industries, API 5L X60 steel is used for storage tanks and pipelines for the transportation and transmission of oil and gas. These steels are in contact with different aggressive environments and are therefore subject to different degrees of corrosion and even cracking. The determination of the absorbed atomic hydrogen makes it possible to assess the susceptibility to hydrogen damage through the outer layers of the pipes. To study the influence of microstructure on the susceptibility to hydrogen absorption in API 5L X60 steel with and without heat treatment at 1050 °C for 30 minutes, the material was characterized by Scanning Electron Microscopy (SEM) and the electrochemical behavior of the metal under simulated CAM conditions, using Potentiodynamic Polarization Curves (PPC) and Oxidation and Hydrogenation Tests. The results indicated a change in the microstructure presenting polygonal grains of β (ferrite), α (perlite) and non-metallic inclusions in the matrix, which generates a significant influence on its ability to absorb atomic hydrogen in the subsurface layers. The kinetics revealed variability in the corrosion potential and passivity mechanism related to the interaction of the microstructure of the material and the chemistry of the solution. In short and intermediate periods of electrochemical charge, a higher corrosion rate is exhibited.

Objetive	Methodology	Contributions
Evaluate the effect of unconventional heat treatment on the electrochemical behavior and susceptibility to hydrogen absorption of API 5L X60 steel under simulated soil conditions from the State of Campeche, Mexico.	Sample preparation and heat treatment. Characterization Microstructure and electrochemistry Results	Understanding the corrosion and passivation mechanisms in this type of steel conditions Simulating soil conditions allows this absorption phenomenon to be studied more realistically.

Hydrogen, Heat treatment, Microstructure, steel, Soil solution

Resumen

El efecto del tratamiento térmico no convencional y el comportamiento electroquímico en el acero API 5L X60 se evalúa mediante procesos/mecanismos electroquímicos asociados con la corrosión. Se evaluó la susceptibilidad a la absorción de hidrógeno en soluciones de suelo representativas del Estado de Campeche, México. En las industrias energética, química, metalúrgica/mecánica y petroquímica, el acero API 5L X60 se utiliza para tanques de almacenamiento y tuberías para el transporte y la transmisión de petróleo y gas. Estos aceros están en contacto con diferentes ambientes agresivos y, por lo tanto, están sujetos a diferentes grados de corrosión e incluso a agrietamiento. La determinación del hidrógeno atómico absorbido permite evaluar la susceptibilidad al daño del hidrógeno a través de las capas externas de las tuberías. Para estudiar la influencia de la microestructura en la susceptibilidad a la absorción de hidrógeno en acero API 5L X60 con y sin tratamiento térmico a 1050 °C durante 30 minutos, se caracterizó el material por Microscopía Electrónica de Barrido (MEB), el comportamiento electroquímico del metal en condiciones CAM simuladas, con Curvas de Polarización Potenciodinámicas (CPP) y Ensayos de Oxidación e Hidrogenación. Los resultados indicaron un cambio en la microestructura presentando granos poligonales de β (ferrita), α (perlita) e inclusiones no metálicas en la matriz, lo que genera una influencia significativa en su capacidad para absorber hidrógeno atómico en las capas subsuperficiales. La cinética reveló variabilidad en el potencial de corrosión y el mecanismo de pasividad relacionado con la interacción de la microestructura del material y la química de la solución. En períodos cortos e intermedios de carga electroquímica se exhibe una mayor tasa de corrosión.

Efecto de los cambios microestructurales asociados al daño por hidrógeno en aceros API 5L X60		
Objetivo	**Metodología**	**Contribuciones**
Evaluar el efecto del tratamiento térmico no convencional sobre el comportamiento electroquímico y la susceptibilidad a la absorción de hidrógeno del acero API 5L X60 en condiciones de suelo simuladas del estado de Campeche, México.	Preparación de muestras y tratamiento térmico Caracterización Microestructural y Electroquímica Resultados	Comprender los mecanismos de corrosión y pasivación en este tipo de condiciones de La simulación de las condiciones del suelo permite estudiar este fenómeno de absorción de forma más realista.

Hidrógeno, Tratamiento térmico, Microestructura, Acero, Solución del suelo

Introduction

API 5L X60 steels have high corrosion resistance and optimal mechanical properties in different environments. This is due to the thermo-mechanical treatment carried out in its manufacturing process. These steels are used as automotive parts, in the manufacture of storage tanks, in the metal-mechanical industry, and in the transportation and conduction of fossil fuels.

Among the main weaknesses of this type of steel is that they are susceptible to hydrogen absorption, a phenomenon that can significantly compromise their structural integrity and cause adverse failures. The effect of absorbed hydrogen on the mechanical properties of steels involves phenomena such as embrittlement, stress corrosion, blistering, delamination or exfoliation[1,2]. It is common practice in industry to minimise the absorption of hydrogen from the environment during this type of process, to avoid its embrittlement that occurs due to a process of absorption and diffusion of hydrogen, when it is incorporated into the crystal lattice permanently or temporarily[3]. The mechanism of hydrogen absorption is shown in Figure 1.

Box 1

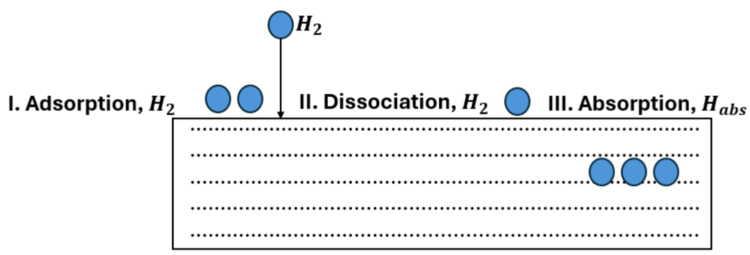

Figure 1
Mechanism of hydrogen absorption[4]

Source: Own elaboration

According to the theory the mechanisms that explain the interaction of hydrogen with iron is manifested by cathodically polarizing and evolving atomic hydrogen from the electrochemical reaction of hydrogen ions or water molecules, these are absorbed through the surface of the material as described in the following reactions[5].

$$H_3O^+ + e^- \leftrightarrow H_{ad} + H_2O \quad (1)$$

$$H_2O + e^- \leftrightarrow H_{ad} + OH^- \quad (2)$$

In equation (1), the hydronium ion (H_3O^+) gain an electron (e^-) resulting in an adsorbed hydrogen atom (H_{ad}) on the surface of the material and at the same time releasing a molecule of water (H_2O). In equation (2), a molecule of water (H_2O) gain an electron (e^-) The extra electron binds to a hydrogen atom in the water, forming a hydride ion (H^-), at the same time a hydroxide ion is released (OH^-). Depending on the reaction conditions, the hydrogen atom adsorbed on the surface of the material (3) can be absorbed or de-absorbed according to the Tafel reaction (4), as observed in the reaction (4).

$$H_{ad} \leftrightarrow H_{ab} \quad (3)$$

$$2H_{ad} \leftrightarrow (H_2)_{ad} \quad (4)$$

In this reaction (4), two hydrogen atoms ($2H_{ad}$) adsorbed hydrogen molecules combine to form an adsorbed hydrogen molecule (H_2). Another possibility of desorption is the Heyrovsky mechanism[4] which also leads to a recombination with hydrogen according to the reaction (5).

$$H_{ad} + H_3O^+ + e^- \leftrightarrow H_2 + H_2O \quad (5)$$

The reaction (5) describes a reduction process in which the hydronium ion (H_3O^+) reduces one electron (e^-) and form water (H_2O). At the same time, the adsorbed hydrogen atom (H_{ad}) combines with other hydrogen to form the molecule of (H_2). The interaction between atomic hydrogen and metals has been extensively researched due to its impact on the properties of materials.

The small dimensión of the hydrogen atom facilitates its penetration and diffusion into metals, especially when combined with the presence of carbon dioxide (CO_2), which accelerates corrosion and degrades protective layers[6].

Experimental Methodology

Materials & Heat Treatment

API 5L X60 steel was used (See Figure 2), with the chemical composition shown in Table 1. Steel was evaluated in arrival condition (MCLMB) and subjected to a heat quenching treatment (MCLTT).

Box 2

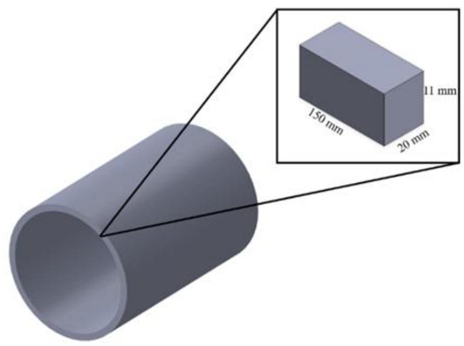

Figure 2
Material Steel API 5L X60

Source: *Own elaboration*

Box 3

Table 1
Chemical composition of API 5L X60 Steel

C	Mn	Si	Al	Nb	Cu	Cr	Ni	Ti	Co
0.067	1.381	0.206	0.023	0.038	0.022	0.016	0.023	0.0094	0.0055

Source: Own elaboration

The analyzed samples were subjected to unconventional quenching, which began with a gradual heating until permanence 1050°C, and for 30 minutes they were kept like this until they were finally quenching in water at room temperature[7,8]. The heat treatment design is shown in Figure 3.

Box 4

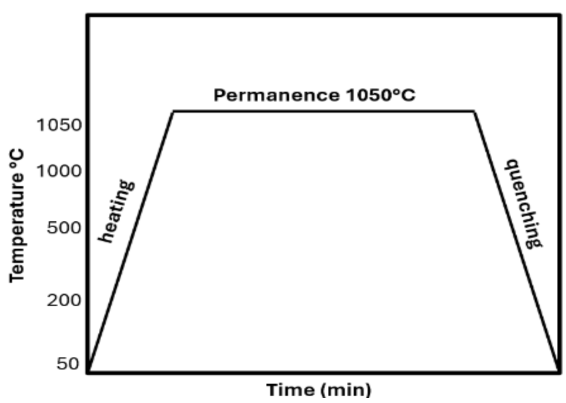

Figure 3
Heat treatment design

Source: *Own elaboration*

Electrochemical Testing

Electrolyte

For the electrochemical tests, the CAM solution was used, which simulates the composition of a soil characteristic of the state of Campeche. The chemical composition of the CAM solution is shown in Table 3[9].

Box 5

Table 2
Chemical Composition of CAM Solution (g/l)

$MgSO_4*7H_2O$	$CaCl_2*H_2O$	KNO_3	$CaCO_3$	$NaHCO_3$
0.0251	0.0215	0.050	0.202	0.823

Source: *Own elaboration*

The composition of the CAM solution shows the main constituents and has a pH of 8.1.

Characterization of the electrochemical behavior of the steels tested

The characterization of the electrochemical behavior of MCLMB and MCLTT in CAM solution was carried out by means of potentiodynamic polarization curves (PPC) and susceptibility to hydrogen damage by means of hydrogenation and oxidation assays. All tests were performed in a conventional three electrode electrochemical cell, MCLMB and MCLTT steels were the working electrodes, a saturated calomel electrode (SCE), as a reference and a graphite bar as an auxiliary electrode. The solution used as an electrolytic medium is representative of the Yucatan Peninsula, Mexico.

Other solutions with alkaline pH have been used to test steels[10,11] but are representative of other locations. To characterize the electrochemical behavior using CPPs, polarization was polarized from -300 mV to 600 mV with respect to the open-circuit potential (OCP), at a speed of 10 mV/min. From these CPP graphs, the aggressiveness of the electrolytic medium and the corrosion rate of MCLMB and MCLTT are determined. All measurements were carried out on a Solartron Potentiostat/Galvanostat. The total amount of hydrogen evolved can be calculated by[12]:

$$Q_H^{ev} \int_0^{\tau_{exp}} I_{cathodic}\,(\tau)d\tau \qquad E_{cathodic} = const \qquad [6]$$

Hydrogenation was performed at constant cathode potential (-200 mV vs Ecorr), at different times and in the absence of oxygen. Hydrogen oxidation was performed by the method described by Yan, M., et al.[11]. The total amount of hydrogen absorbed sub-superficially by the metal can be defined through equation[8]:

$$Q_H^{abs} = \int_0^{\tau_{des}} \left[I_H(\tau) - I_{ref}(\tau)\right] d\tau \qquad E_{anodic} = const \qquad [7]$$

Where $I_H(\tau)$ is the anodic bias current for the sample charged with hydrogen and $I_{ref}(\tau)$ is the anodic bias current for the sample without hydrogenation. For the quantification of absorbed hydrogen (H_{abs}), Equation 8 was used for the samples tested.

$$C_H = \frac{Q_H^{abs}}{zFv} \qquad [8]$$

Where, z is the number of electrons participating in the reaction, F is Faraday's constant, and v is the effective volume of the sample.

Results

Microstructural characterization of the steels tested

Figure 4 shows a micrograph of MCLMB, the main phases that were identified were polygonal ferrite (α) and perlite (β), characteristics of API 5L X60 steels. Non-metallic inclusions were also randomly found in the steel matrix, ranging in size from 3 to 50 μm. In recent research, Velázquez et al. revealed that non-metallic inclusions have a role in pitting corrosion directly, causing defects in the microstructure. Inclusions with smaller areas were observed that tend to be more prone to corrosion than larger inclusions. However, it seems that elongated inclusions are more active than circular inclusions because the proportion of inclusions to active starts is higher than that of circular ones[13].

Box 6

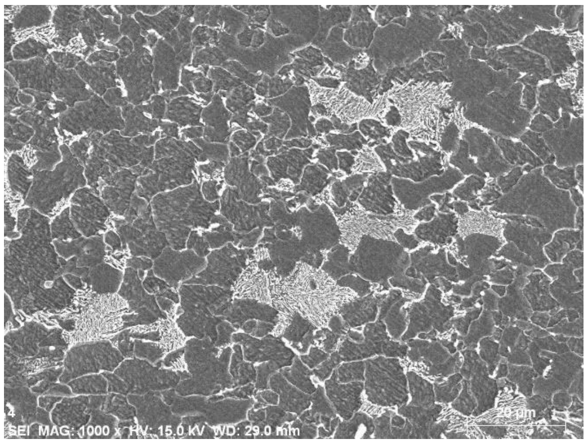

Figure 4

MCLMB Steel Microstructure

Source: *Own elaboration*

The inclusions identified in MCLMB steel are rich in silicon (Si), Aluminium (Al), Magnesium (Mg) and Calcium (Ca), although they may be present as complexes of O-Al-Mg-Ca[13]. Inclusions consist of one or several deformed or non-deformed thin parts, deformed thin parts are mainly low-melting calcium aluminates, while non-deformed particles contain more CaS o CaO y Al_2O_3 high melting point[14]. The main elements that exist in inclusions are Al, O, Ca, Mg, Mn y C, as well as complexes or mixes Al-Mg-Ca-O. The interfaces of non-metallic and precipitated inclusions are considered strongly irreversible traps for hydrogen at normal temperatures and conditions[14].The microstructure of MCLTT steel is characterized phases of bainite and ferrite. The microstructure of MCLTT steel increases the mechanical properties with more diverse phases in the matriz.

Electrochemical behavior of MCLMB and MCLTT steel, in CAM solution

Figure 5 shows the CPPs of MCLMB and MCLTT steels in CAM solution. In PPCs, it is observed that MCLMB steel exhibits a more negative corrosion potential, and a higher corrosion current density compared to MCLTT[15]. However, MCLMB steel is more susceptible to corrosion, due to the formation of corrosion products and the dissolution of the phases present by the chemistry of the solution[13. The] two metallurgical conditions tested show a controlled process by charge transfer, indicating that they are susceptible to corrosion in CAM solution. MCLTT steel revealed greater corrosion resistance, with a nobler corrosion potential and lower current densities[15]. The corrosion rates for MCLMB and MCLTT specimens are 2.42 mm/year and 1.9 mm/year, respectively. This behavior can be attributed to the fact that heat treatment can produce a protective effect against grain regrouping corrosion in steel[16].

Box 7

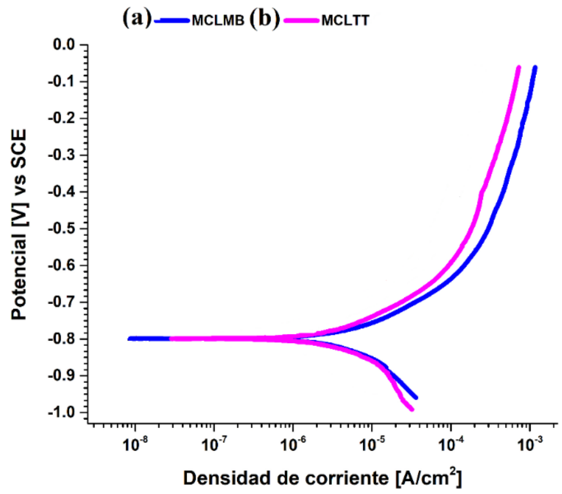

Figure 5
CPP of MCLMB (a) and MCLTT (b) steel, in CAM solution

Source: *Own elaboration*

Behavior of the cathodic and anodic current density associated with hydrogen

The current time series associated with the evolution of atomic hydrogen can be statistically analyzed to give us information on the behavior of the hydrogen-metal interaction. Electrochemical noise is defined as low-frequency (<10 Hz) and low-amplitude potential or current fluctuations, originating from natural electrochemical variations of corrosive kinetics. Electrochemical noise under potentiostatic and galvanostatic control[17] has been used to interpret corrosive processes in stainless steels[18], processes associated with the evolution of hydrogen[19,20].

Figure 6 shows the behavior of the average current density of the MCLMB and MCLTT. The MCLMB sample shows an overall increase in cathodic current density over time, although with some fluctuations. This suggests that the rate of the reduction reaction increases over time. On the other hand, it was observed that MCLTT steel also shows an overall increase in current density, but with a slightly lower slope than MCLMB. In addition, it has a more marked fluctuation around 10 hours. The differences in the behavior of the two metallurgical conditions are attributed to different electrochemical processes that occur on the surface of each of the steels tested. These processes may include the adsorption of chemical species, the formation of passive films, or more complex reactions[19].

Box 8

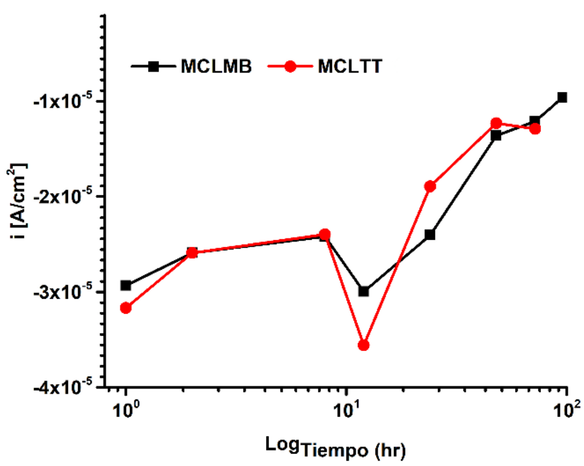

Figure 6
Behavior of the average current density of MCLMB and MCLTT in CAM solution.

Source: *Own elaboration*

On the other hand, heat treatment generates different phases, among which are: bainite, acicular ferrite, globular ferrite, Widmanstatten ferrite.

On the contrary, the base metal has ferrite and perlite as its main phases, in these phases the average cathodic current density tends to decrease with increasing assay time, this is in accordance with the cathodic protection mechanism, since the entire surface inhibits the anode and cathode sites that could cause the average current density to vary widely, this is due to the cathodic potential applied. Figure 7 shows the concentration of atomic hydrogen (AC) and the permeation coefficient of the steels in CAM solution.

Box 9

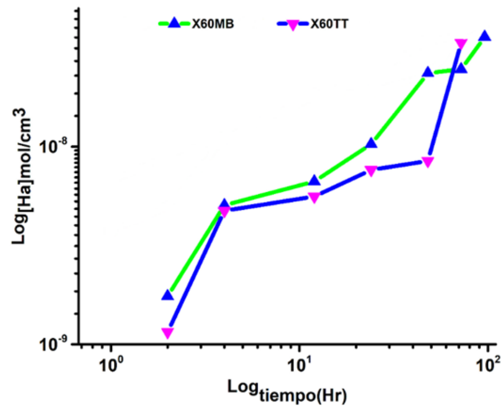

Figure 7
Hydrogen concentration in MCLMB (a) and MCLTT (b) steels

Source: *Own elaboration*

MCLMB steel shows a higher susceptibility to sup-surface atomic hydrogen adsorption compared to MCLTT steel in the first hours of electrochemical charge, although it always tends to increase with longer test times. In the 48 hours of electrochemical charge MCLMB steel almost equals the concentration of adsorbed atomic hydrogen as MCLTT steel, this behavior may be due to a slower process kinetics in MCLTT steel. The higher absorption capacity of atomic hydrogen in MCLMB steel is mainly due to the microstructure constituted by ferrite-perlite interfaces, grain boundaries and non-metallic inclusions[20]. Unlike MCLTT steel which absorbs less atomic hydrogen compared to non-heat-treated steel according to the concentration of absorbed hydrogen (Ha).

Previous research by Park, G. T.[21], has shown that the presence of an acicular bainite-ferrite structure, mainly associated with Acicular Ferrite, is characterized by randomly oriented grain boundaries and a high density of dislocations. Due to the complex and entangled network of dislocations, atomic hydrogen is trapped in reversible traps (dislocations), decreasing absorption and consequent diffusion into the volume of the steel. It was observed that MCLTT steel has a lower concentration of hydrogen compared to MCLTT steel. This suggests that heat treatment is more effective in reducing hydrogen diffusion. The difference in hydrogen concentration between heat-treated and non-heat-treated steels becomes more apparent at longer exposure times.

Figure 8 shows the behavior of the permeation coefficient of MCLMB and MCLTT steels, this parameter does not indicate the sup-surface absorption efficiency of the steels tested[19]. Initially, MCLMB steel has a permeation coefficient higher than X60MCLTT. However, over time, this difference narrows. This indicates that heat treatment could give the steel a lower initial permeability to hydrogen, but in the long term, both alloys tend to behave similarly.

It was observed that, during the first hours of exposure, a maximum was reached for MCLMB steel and in the four-hour test for MCLTT steel. Subsequently, both types of steel show an overall decrease in the permeation coefficient as exposure time increases. This suggests that, over time, steel become less permeable to hydrogen, this may be due to atomic hydrogen saturation in the subsurface film of the steels[21].

Box 10

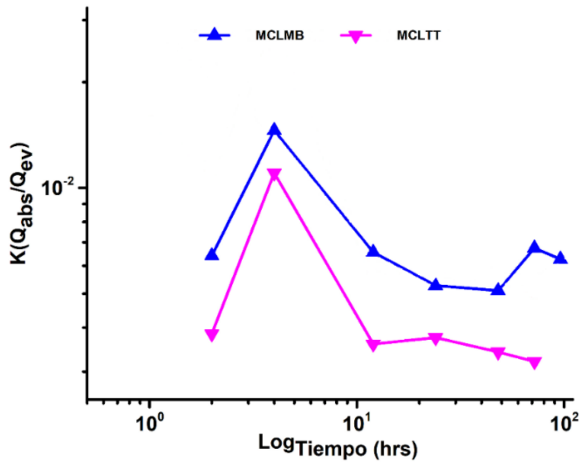

Figure 8
Permeation coefficient behavior in MCLMB and MCLTT steels.

Source: Own elaboration

Hydrogen saturation on the metal surface, which exceeds its solubility limit, is the main cause of the decrease in the K-coefficient as the hydrogenation process progresses. This coefficient, which initially reaches high values, reflects the intense electrochemical activity that occurs in the early stages[19].

Conclusiones

MCLMB and MCLTT steel showed susceptibility to subsurface hydrogen absorption in the CAM solution. At short and medium electrochemical charge times it shows aggressiveness and tends to increase the concentration of hydrogen. This indicates the need for longer hydrogenation times to be able to observe behavior comparable to real operating situations.

The microstructure has a significant influence on the susceptibility to subsurface absorption of atomic hydrogen, since in the two solutions tested it tends to absorb less hydrogen, although a more in-depth study and analysis of the influence of heat treatment is necessary.

Declarations

Conflict of interest

The authors declare that they have no conflict of interest. They have no financial interests or personal relationships that could have influenced this book.

Authors' contribution

Calan-Canche, Damian: Main author of research topic, contribution to methodology and analysis of results.

Reda-Cruz, Alfredo: Review of research methodology.

Gonzalez-Sanchez, Jorge: Contribution to the subject of research, review of methodology and analysis of results.

Flores-Chan, J. E.: Analysis of results

Availability of data and materials

The data and materials used in this study are available.

Financing

No financing

References

Antecedents

Uribe Pérez, I., et.al (2011). Fundamentals of hydrogen damage in steels. Man, and Machine, pages 2-5.

Thompson, A W, & Bernstein, I M (1976). Effect of hydrogen on behavior of materials.

M. Barteri, F. Mancia, A. (1987) Engineering diagrams and sulphide stress corrosion cracking of duplex stainless steels in deep sour well environment. Corrosion Science, pages 1-5.

Truschner, M., Trautmann, A., & Mori, G. (2021). The basics of hydrogen uptake in iron and steel. BHM Berg-und Huttenmannische Monatshefte, pages 1-7.

E. G. Dafft, K.B.a.H.J.E., (1999). Investigations of hydrogen evolution kinetics and hydrogen absorption by iron electrodes during cathodic polarization. Corrosion Science, pages 1-7.

Linter, B. ., y Burstein, G. . (1999). Reactions of pipe steels in carbon dioxide solutions. Corrosion Science, 41(1), 117–139.

Basics

Niu, L., Cheng, Y.F., (2007), Mechanism for hydrogen evolution reaction on pipeline steel in near-neutral pH solution. Electrochemistry Communications, pages 1-5.

B.R. Linter, G.T.B., (1999), Reactions of pipelines steels in carbon dioxide solutions. Corrosion Science, pages 1-9.

ASTM, Designation: E407-07, “Standard Practice for Microetching Metals and Alloys”, 2015.

Noor, E.A., (2011) Comparative analysis for the corrosion susceptibility of Cu, Al, Al-Cu and C-Steel in soil solution. Materials and Corrosion, pages. 1-4.

K. Belmkre, N.A., F. Kermiche, M. Wery and J. Pagetti, (1998) Corrosion study of carbon steel protected by a primer, by electrochemical impedance spectroscopy (EIS) in 3% NaCl medium and in a soil simulating solution. Materials and Corrosion: pages. 1-4.

Maocheng Yan, Y.W. (2006) Study on hydrogen absorption of pipeline steel under cathodic charging. Corrosion Science, pages. 1-4.

Support

Velázquez, J.C. et.al (2023) Study on the Influence of Non-Metallic Inclusions on the Pitting Corrosion of API 5L X60 Steel. Coatings 2023, pages1-10

Xinhua Wang, X.L., Qiang Li, Fuxiang Huang, Haibo Li, and Jian Yang (2014). Control of stringer shaped non-metallic inclusions of CaO-Al2O3 system in API X80 linepipe steel plates. Steel research international pages. 1-9.

Discussions

Luo Jinheng, Z.L., et al. (2016). Electrochemical corrosion behaviors of the X90 linepipe steel in NS4 solution. Natural Gas Industry B. pages. 1-3.

Luo Jinheng, Z.L., Li Lifeng, Yang Fengping, Ma Weifeng, Wang Ke, Zhao Xinwei25. Electrochemical corrosion behaviors of the X90 linepipe steel in NS4 solution. Natural Gas Industry B, 2016. 3: p. 346-351.

L. Zhang, M.D., and Y. Li, (2012) Effects of Aplied Potentials on the Hydrogen-Induced Cracking of Pipeline Steel in Low-Temperature and Low-Disolved-Oxigen Seawater. Corrosion. pages 1-5.

Cheng, Y.F., (2007). Fundamentals of hydrogen evolution reaction and its implications on near-neutral pH stress corrosion cracking of pipelines. Electrochemical Acta, pages.1-5.

Gyu Tae Park, S.U.K., Hwan Gyo Jung, Kyo Young Kim. Effect of microstructure on the hydrogen trapping efficiency and hydrogen induced cracking of linepipe steel. Corrosion Science, pages 1-4.

Benítez, José Luis, Lárez Velásquez, Cristóbal, & Rojas de Gáscue, Blanca. (2015). Cinética de absorción y transporte del agua en hidrogeles sintetizados a partir de acrilamida y anhídrido maleico. Revista Latinoamericana de Metalurgia y Materiales, pages 1-4.

R.K. Gupta, N.L. Sukiman, M.K. Cavanaugh, B.R.W. Hinton, C.R. Hutchinson, N. Birbilis, (2012). Metastable pitting characteristics of aluminium alloys measured using current transients during Potentiostatic polarisation. Electrochimica Acta. 66 245–254.